Green Chemistry

Dynamic Article Links ▶

PAPER

High-temperature synthesis of strong acidic ionic liquids functionalized, ordered and stable mesoporous polymers with excellent catalytic activities†

Fujian Liu, Shufeng Zuo, Weiping Kong and Chenze Qi*

Strong acidic ionic liquids functionalized, ordered and stable mesoporous phenol–formaldehyde resins (OMR-ILs) monoliths have been successfully synthesized from the treatment of ordered mesoporous resins (OMR-[HMTA]) using 1,3-propanesultone, followed by ion exchanged using various strong acids. The OMR-[HMTA] samples could be synthesized by the assembly of block copolymer template of F127 with preformed resol, which could be obtained from heating a mixture of phenol and formaldehyde at 70 °C; during curing processes, certain contents of the hexamethyltetramine (HMTA) cross linker were also introduced, after hydrothermal treatment at 200 °C for 20 h, calcination at 360 °C under nitrogen, OMR-[HMTA] samples with opened mesopores were obtained. Characterizations suggest that OMR-ILs have ordered and stable mesospores, high BET surface areas, and strong acid strength. Interestingly, OMR-ILs show much higher catalytic activities and recyclability in the esterification of acetic acid with cyclohexanol, hydration of propylene oxide, Peckmann reaction of resorcinol with ethyl acetoacetate and transesterification of tripalmitin with methanol than those of Amberlyst 15, sulfonic group functional ordered mesoporous silicas and acidic zeolites, which were even comparable with that of H_2SO_4. The unique features of OMR-ILs such as superior thermal stability, excellent catalytic activities and recyclability, will be potentially important for their applications in industry.

Introduction

Ordered mesoporous materials have been paid much attention since the first discovery of M41S in 1992 by Mobile scientists,[1,2] which showed the unique structural properties including high BET surface areas, uniform and adjustable mesopores, tunable periodic structures and versatile compositions.[2] Typically ordered mesoporous materials were silica, metal oxides, carbons and resins, which having been widely used in the fields of separation, adsorption, catalysis, heat insulators and host–guest functional materials.[3–10]

In the last few years, Zhao *et al.* have successfully synthesized a family of ordered mesoporous phenol–formaldehyde polymers (FDU type resins)[9,11–15] with versatile mesostructures using block copolymer templates of P123 or F127 at low temperatures ranging from 70 to 100 °C, which ignites the research interests and offers great opportunities for applying the ordered mesoporous polymers as functional materials in the field of biological reactors, sensors, selective membranes, heat insulators, and catalysts or catalyst supporters.[9,16–18] Following the pioneering work of Zhao *et al.*, Xing *et al.* reported the first use of ordered

mesoporous phenol–formaldehyde resins (FDU-14, -15) on heterogeneous acid catalysis by grafting sulfonic groups onto the network of FDU-14 or FDU-15, giving very good catalytic activities in the liquid-phase Beckmann rearrangement of cyclohexanone oxime and the condensation of bulky aldehydes with alcohols,[19] which opens a new way for applications of ordered mesoporous polymers on heterogeneous acid catalysis, attributing to their advantages of easy separation of the catalyst from the reaction medium, reductive corrosion, improved regenerability, and enhanced product selectivity as compared with that of mineral acids.[20–34]

As a typical heterogeneous acid catalysts, the grafting of strong acidic ionic liquids (ILs) onto porous materials such as mesoporous silicas and zeolites[35–37] have received considerable attention due to their unique features including high BET surface areas, strong acid strength, highly exposed degree of active sites, resulting in their excellent catalytic activities in various acid-catalyzed reactions, which offers great opportunities for the wide application of ILs as green and renewable heterogeneous catalytic materials. However, the hydrophilic inorganic networks of the supporters largely effect their catalytic activities due to water, usually as a by-product, in many acid catalyzed reactions, which easily co-adsorb near the acidic sites, further leading to the partial deactivation or leaching of the active sites.[38,39] Moreover, the presence of organic halides containing the cation usually results in the destroying of the inorganic supporters, which largely constrains their wide applications.[40]

Institute of Applied Chemistry, Shaoxing University, Shaoxing, 312000, People's Republic of China. E-mail: qichenze@usx.edu.cn; Fax: +86-575-88345681; Tel: +86-575-88345681

Compared with porous inorganic supporters, porous polymers showed adjustable hydrophobicity and good stability for various acids. Up to now, there were still no reports on immobilization of acidic ILs onto ordered mesoporous polymers. We demonstrate here a high temperature (200 °C) hydrothermal synthesis of strong acidic ionic liquids functionalized, ordered and stable mesoporous resins (OMR-ILs) for the first time, the high synthesis temperature will be helpful for obtaining the samples with a high cross-linking degree, resulting in their extra-ordinary thermal and mechanical stabilities as compared with the samples (FUD type of mesoporous polymers) synthesized at lower temperature (≤100 °C).[41–45] Generally, the synthesis of OMR-ILs was carried out by treating hexamethyltetramine (HMTA) cross-linked ordered and stable mesoporous resin (OMR-[HMTA]) using 1,3-propanesultone, ion exchanging using various strong acids. The performed OMR-[HMTA] could be synthesized from the self assembly of copolymer template of F127 with resol in the presence of hexamethyltetramine (HMTA) cross-linker under high temperature hydrothermal conditions. Notably, the obtained OMR-ILs exhibited ordered and stable networks, high BET surface areas, adjustable hydrophobicity, and strong acid strength, resulting in OMR-ILs exhibiting extra-ordinary catalytic activities and recyclability in various acid-catalyzed reactions, including esterification of acetic acid with cyclohexanol, hydration of propylene oxide, Peckmann reaction of resorcinol with ethyl acetoacetate and transesterification of tripalmitin with methanol as compared with conventional solid acid catalysts of Amberlyst 15, ionic liquids functional mesoporous SBA-15 and acidic zeolites, which were even comparable with that of H_2SO_4.

Experimental

Chemicals and reagents

All reagents were of analytical grade and used as purchased without further purification. Nonionic block copolymer template poly(ethyleneoxide)–poly(propyleneoxide)–poly(ethyleneoxide) (Pluronic F127, molecular weight of about 12 600), tripalmitin, Amberlyst 15 were purchased from Sigma-Aldrich Company, Ltd (USA). Phenol, formaldehyde solution (37 wt%), NaOH, HMTA, methanol, propylene oxide, acetic acid, cyclohexanol, resorcinol, ethyl acetoacetate, toluene, CH_2Cl_2, 1,3-propanesultone, trifluoromethanesulfonic acid, sulfuric acid were obtained from Tianjin Guangfu Chemical Reagent. H-form of Beta zeolite and ultrastable Y zeolite (USY) were supplied by Sinopec Catalyst Co.

Synthesis of OMR-[HMTA]

OMRs were hydrothermally synthesized at 200 °C from the self-assembly of resol precursors, cross-linker of HMTA and block copolymer template of F127 with a molar ratio of C_6H_5OH–CH_2O–NaOH–F127–HMTA–H_2O at 1 : 4.34 : 0.235 : 0.0093 : 0.17 : 90.6. As a typical run, 2.0 g of phenol and 7 mL of a formaldehyde solution (37 wt%) were dissolved in 10 mL of a 0.5 M NaOH solution, and were stirred at 72 °C for 30 min. Then, a solution containing 2.5 g of F127 ($EO_{106}PO_{70}EO_{106}$, M_w = 12 600) and 20 mL of deionized water was added, in the meanwhile, 0.5 g of HMTA was introduced into the mixture as additional cross-linker, after stirring at 78 °C for an additional 3 h, the mixture was transferred into an autoclave for further curing at the temperature of 200 °C for 24 h, a brown solid could be found at the bottom of the autoclave, after filtration, washing with a large amount of water, drying at 80 °C, OMR-[HMTA] was obtained. The OMR-[HMTA] with open mesopores can be obtained by calcining at 360 °C for 5 h in nitrogen gas containing a small amount (2.5%, v/v) of oxygen or by washing with ethanol for 48 h under reflux.

Synthesis of OMR-ILs

OMR-ILs were synthesized through the treatment of OMR-[HMTA] using 1,3-propanesultone, which makes the nitrogen in the network formation of quaternary ammonium salt, followed by ion exchanging with various strong acids. As a typical run for the synthesis of OMR-[C_3HMTA][SO_3CF_3], 0.5 g of OMR was dispersed into 10 mL of toluene, then 0.5 g of 1,3-propanesultone was added, the temperature was rapidly increased to 100 °C, the reaction lasted for 24 h. After cooling to room temperature, the resulting sample was washed with toluene and then a large amount of CH_2Cl_2, and was then dried at 80 °C for 6 h to yield OMR-[C_3HMTA].

The obtained sample was then dispersed into 10 mL of toluene, then 4.5 mL of HSO_3CF_3 was added, after further stirring at room temperature for 24 h, the sample was washed with toluene and a large amount of CH_2Cl_2 to remove the surface adsorbed acids, OMR-[C_3HMTA][SO_3CF_3] was obtained. Except for HSO_3CF_3, other acids such as H_2SO_4, HBF_4 etc., can also be chosen as the exchange acids.

In comparison, SBA-15-[C_3mim][SO_3CF_3] and SBA-15-Ar-SO_3H were synthesized according to the literature.[33,46,47]

Characterizations

X-Ray diffraction (XRD) patterns were recorded on Rigaku D/Max-2550 using nickel-filtered Cu Kα radiation. N_2 isotherms were measured using a Micromeritics ASAP Tristar system at the liquid nitrogen temperature. The samples were outgassed for 10 h at 150 °C before the measurements. The pore-size distribution for mesopores was calculated using the Barrett–Joyner–Halenda (BJH) model. CHNS elemental analysis was performed on a Perkin-Elmer series II CHNS analyzer 2400. FTIR spectra were recorded by using a Bruker 66V FTIR spectrometer. XPS spectra were performed on a Thermo ESCALAB 250 with Al Kα radiation, and binding energies were calibrated using the C1s peak at 284.9 eV. Transmission electron microscopy (TEM) experiments were performed on a JEM-3010 electron microscope (JEOL, Japan) with an acceleration voltage of 300 kV. Thermogravimetric analyses (TG) were performed on a Perkin-Elmer TGA7 in flowing air with the heating rate of 20 °C min^{-1}. The acidity of the samples was measured by ammonia adsorption and temperature-programmed desorption (NH_3–TPD) technique. Typically, 0.2 g of sample (40–60 mesh) was saturated with NH_3 at 100 °C. Then, the sample was purged by Ar flow to remove the physically adsorbed ammonia on the sample. Finally desorption of NH_3 was carried out from 100 to 600 °C with a heating rate at 20 °C min^{-1}.

Catalytic reactions

Esterification of acetic acid with cyclohexanol (EAC) was performed by the mixing and stirring of 0.2 g of catalyst and 11.5 mL (0.11 mol) of cyclohexanol in a three-necked round flask equipped with a condenser and a magnetic stirrer. After heating the mixture to 100 °C by oil bath, 17.5 mL (0.305 mol) of acetic acid was rapidly added, the reaction was kept at 100 °C for 5 h. In this reaction, the molar ratio of acetic/cyclohexanol acid was 2.6 and the mass ratio of catalyst/cyclohexanol was 0.018. The product was cyclohexyl acetate with selectivity for near 100%.

The Peckmann reaction of resorcinol with ethyl acetoacetate (PRE) was performed by the mixing and stirring of 0.2 g of catalyst, 10 mmol of resorcinol and 10 mmol of ethyl acetoacetate in a glass flask equipped with a condenser and a magnetic stirrer, then 10 mL toluene as solvent was added, then the temperature was increased to 110 °C and lasted for 2 h. The molar ratio of resorcinol/ethyl acetoacetate was 1.0 and the mass ratio of catalyst/ethyl acetoacetate was 0.154.

Transesterification of tripalmitin with methanol (TTM) was performed as follows: 0.84 g (1.04 mmol) of tripalmitin was added into a three-necked round flask equipped with a condenser and a magnetic stirrer, then the temperature was increased to 65 °C. After the tripalmitin melted, 4.93 mL of ethanol and 0.05 g of catalyst were quickly added under strong stirring, the reaction was kept at 65 °C for 8 h. The molar ratio of tripalmitin/methanol was 1 : 120 and the mass ratio of catalyst/tripalmitin was 0.0595. The product was methyl palmitate with a selectivity of nearly 100%.

Hydration of propylene oxide (HPO) was performed by the mixing and stirring of 0.1 g of catalyst, 50 mmol of propylene oxide, 500 mmol of H_2O in a glass flask equipped with a condenser and a magnetic stirrer. The reaction lasted for 6 h at 27 °C under stirring. The molar ratio of propylene oxide/water was 0.1 and the mass ratio of catalyst/water was 0.011. The product was 1,2-propylene glycol with a selectivity of nearly 100%.

All the reactions were analyzed by gas chromatography (Agilent 7890) with a flame ionization detector (FID) and dodecane as an internal standard. The column was HP-INNO-Wax capillary column (30 m); the initial temperature was 100 °C, temperature rate was 20 °C min⁻¹, and final temperature was 280 °C; the temperature of the FID detector was 300 °C.

Results and discussion

Fig. 1 shows the small angle X-ray diffraction (XRD) patterns of OMR-[HMTA], OMR-[C_3HMTA][SO_4H], and OMR-[C_3HMTA][SO_3CF_3]. Clearly, all the samples showed three obvious diffraction peaks indexed as (110), (200) and (211) reflections associated with the body-centered cubic space group of ($Im\bar{3}m$),[48] indicating a highly ordered mesostructure. For OMR-[HMTA], giving d value of (110) direction at 9.6 nm, after functionalized with strong acidic ionic liquids resulting in OMR-[C_3HMTA][SO_4H] and OMR-[C_3HMTA][SO_3CF_3], giving relative lower d values of (110) direction at 9.2 and 9.0 nm respectively, which maybe due to the block of the mesopores by ionic liquids functional groups on the OMR-[HMTA] sample.
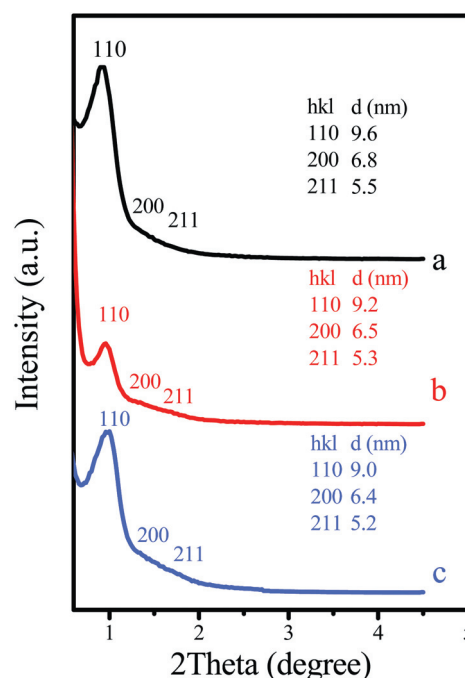

Fig. 1 Small angle XRD patterns of (a) OMR, (b) OMR-[C_3HMTA][SO_4H] and (c) OMR-[C_3HMTA][SO_3CF_3].
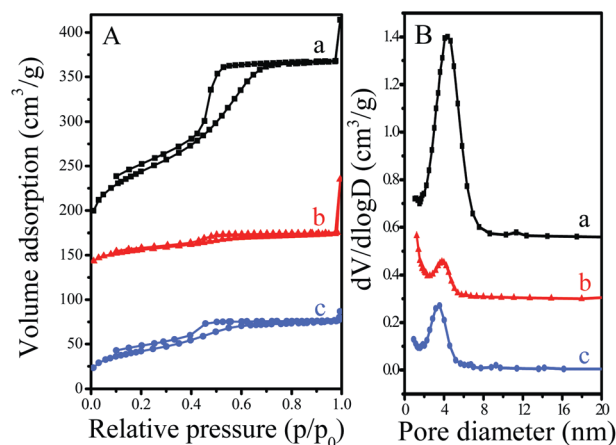

Fig. 2 (A) N_2 adsorption–desorption isotherms and (B) the corresponding pore size distribution of (a) OMR, (b) OMR-[C_3HMTA][SO_4H] and (c) OMR-[C_3HMTA][SO_3CF_3]. The isotherms for (a) and (b) were offset by 150 and 100 cm³ g⁻¹ along with vertical axis for clarity, and pore size distribution for (a) and (b) were offset by 0.4 and 0.3 cm³ g⁻¹ along with vertical axis for clarity, respectively.

Fig. 2 shows the N_2 isotherms and the correspondingly pore size distribution of OMR-[HMTA], OMR-[C_3HMTA][SO_4H] and OMR-[C_3HMTA][SO_3CF_3]. Clearly, all the samples exhibit type-IV curves with a sharp capillary condensation step at p/p_0 = 0.4–0.6 with a H2-type hysteresis loops (Fig. 2A), which were characteristic of a 3D caged mesostructure.[48] Interestingly, compared with OMR-[HMTA], OMR-[C_3HMTA][SO_4H] and OMR-[C_3HMTA][SO_3CF_3] showed relatively lower BET surface areas, pore volumes and smaller pore sizes. For example, OMR-[HMTA] showed the BET surface area of 339 m² g⁻¹, pore

Table 1 The textural and acidic parameters of various solid acid catalysts

Samples	Acid sites[a] (mmol g^{-1})	S content[b] (mmolg^{-1})	Textural parameters		
			S_{BET} (m^2 g^{-1})	V_P (cm^3 g^{-1})	D_P[c] (nm)
OMR	—	—	339	0.40	4.4
OMR-[C$_3$HMTA][SO$_4$H]	1.91	1.64	194	0.21	3.8
OMR-[C$_3$HMTA][SO$_3$CF$_3$]	1.30	1.17	152	0.15	3.5
Amberlyst 15	4.70	4.3	45	0.31	40.0
SBA-15-Ar-SO$_3$H	1.34	1.22	626	0.72	6.3
SBA-15-[C$_3$mim][SO$_3$CF$_3$]	0.78	0.82	589	0.76	5.7
H-USY[d]	2.06	—	623	0.26	14.7
H-Beta[e]	1.21	—	550	0.20	0.67
H$_2$SO$_4$	20.4	10.2	—	—	—

[a] Measured by acid–base titration. [b] Measured by elemental analysis. [c] Pore size distribution estimated from BJH model. [d] Si/Al ratio at 7.5. [e] Si/Al ratio at 12.5.

Fig. 3 TEM images of (A) OMR viewed from different directions, and (B), (C), (D) of OMR-[C$_3$HMTA][SO$_4$H] viewed from (110), (111) and (100) directions.

volume of 0.40 cm^3 g^{-1} and pore size of 4.4 nm; on the contrary, OMR-[C$_3$HMTA][SO$_4$H] and OMR-[C$_3$HMTA][SO$_3$CF$_3$] showed the relative lower BET surface areas of 194 and 152 m^2 g^{-1}, lower pore volumes of 0.21, 0.15 cm^3 g^{-1} and smaller pore size distribution of 3.8 and 3.5 nm (Table 1). The decreases in the BET surface areas and pore sizes of OMR-ILs were attributed to the introduction of ionic liquid groups onto the framework of the polymers, resulting in blocks of mesopores and increased weight of the OMR-[HMTA] samples' network, giving relatively lower BET surface areas and smaller pore sizes. Similar results have been reported previously,[38] which were much higher than that of Amberlyst 15 (Table 1, 45 m^2 g^{-1}), and lower than that of SBA-15-[C$_3$mim][SO$_3$CF$_3$] (Table 1, 589 m^2 g^{-1}). Additionally, the content of the acid sites of OMR-[C$_3$HMTA][SO$_4$H] and OMR-[C$_3$HMTA][SO$_3$CF$_3$] are 1.91 and 1.30 mmol g^{-1} (Table 1), which were higher than that of SBA-15-Ar-SO$_3$H (1.34 mmol g^{-1}, Table 1) and SBA-15-[C$_3$mim][SO$_3$CF$_3$] (0.78 mmol g^{-1}, Table 1), and lower than that of Amberlyst 15 (4.70 mmol g^{-1}, Table 1).

Fig. 3 shows TEM images of the OMR-[C$_3$HMTA][SO$_4$H] sample. The low-magnification image shows highly ordered mesopores (Fig. 3A). Moreover, the sample exhibits highly ordered areas of (110), (111) and (100) incidences (Fig. 3B, C and D),[44] corresponding to the cubic symmetry ($Im\bar{3}m$), which is in good agreement with the small angle XRD results.

Fig. 4 shows the XPS spectra of OMR-[C$_3$HMTA][SO$_4$H], which exhibited the signals of S2p, S2s, C1s, N1s and O1s. The S2p and S2s peaks at 169.1 and 234.3 eV are assigned to S–O and S=O bonds; C1s peaks at 284.7 and 286.4 eV are associated with C–C and C–S bonds;[49] the signal of N1s came from the cross-linker of HMTA. Notably, the peak around 402 eV results from the quaternized nitrogen by 1,3-propanesultone, suggesting successful quaternization of the nitrogen element onto the network of OMR-[HMTA],[49] indicating the successful introduction of sulfuric based ionic liquid group onto the network of OMR-[HMTA].
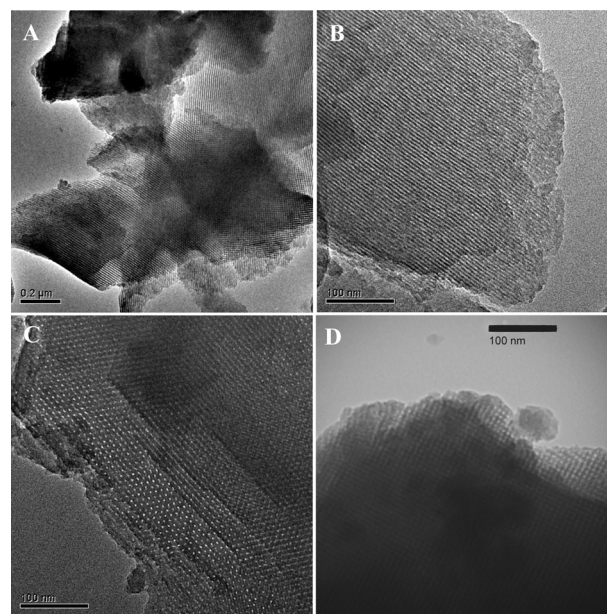
Fig. 5 shows the FT-IR spectra of OMR-[C$_3$HMTA][SO$_4$H] and OMR-[C$_3$HMTA][SO$_3$CF$_3$]. For both samples, the bands around 613, 1032 and 1180 cm^{-1} are associated with the signals of C–S and S=O bonds, demonstrating the successfully functionalization of OMR-[HMTA] by sulfonic group based ionic liquids,[35,36,38] in good agreement with the results of XPS. Moreover, for OMR-[C$_3$HMTA][SO$_3$CF$_3$], except for the signals of sulfonic group, the new bands around 1257 and 1401 cm^{-1} are associated with C–F bond, further confirming the successfully introduction of SO$_3$CF$_3$ group onto the network of OMR-[C$_3$HMTA][SO$_3$CF$_3$].[50]

Fig. 6 showed the TG curves of conventional acidic resin of Amberlyst 15 and OMR-[C$_3$HMTA][SO$_3$CF$_3$]. Notably, both of the samples exhibited the weight loss at temperatures between 250–470, and 480–600 °C, which are mainly attributed to the decomposition of the acidic groups and destruction of the polymer network respectively.[51,52] Interestingly, the decomposition temperature of both the functional groups (385 °C) and network (548 °C) of OMR-[C$_3$HMTA][SO$_3$CF$_3$] were higher than those of Amberlyst 15 (310 and 528 °C), demonstrating OMR-[C$_3$HMTA][SO$_3$CF$_3$] was stable enough below the temperature of 340 °C. Considering the different stabilities of functional groups and the network between OMR-[C$_3$HMTA][SO$_3$CF$_3$] and Amberlyst 15, the stable network of OMR-[C$_3$HMTA][SO$_3$CF$_3$] was mainly attributed to its high cross-linking degree. It was worth noting that the stable network may be favorable for constraining the decomposition of the functional groups into its mesopores as compared with the functional groups immobilization on the supporters with poor porosity,[38] further resulting in their relatively high thermal stability. Moreover, the presence of the strong electron withdrawing group, –SO$_3$CF$_3$, in the mesopores of OMR-[C$_3$HMTA][SO$_3$CF$_3$] would be also helpful for improving the stability of polymeric network to some extent.[40–43,53] The superior stability of OMR-
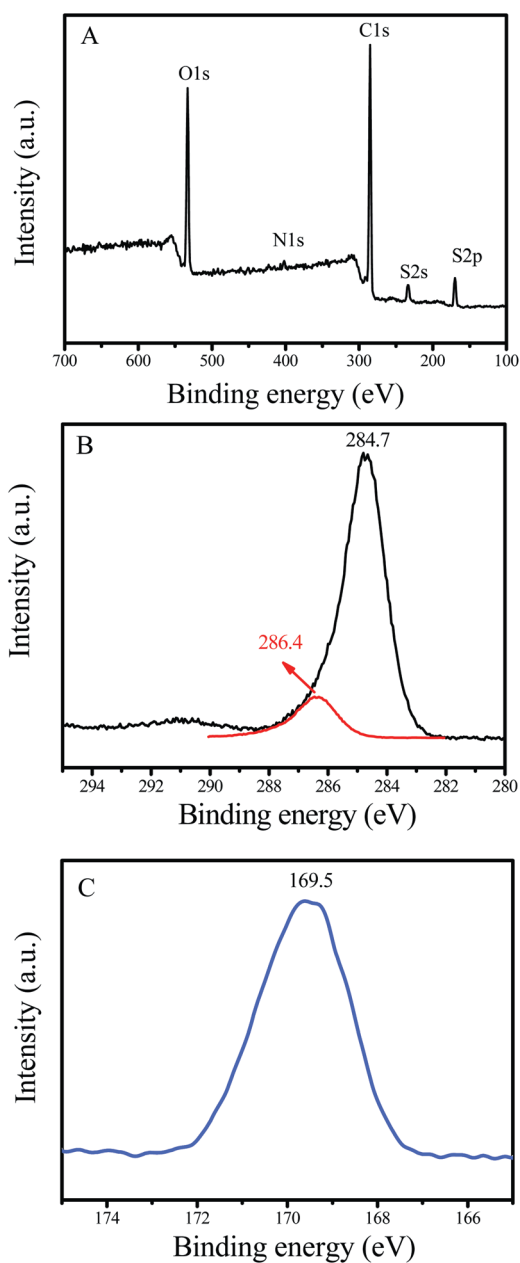
Fig. 4 XPS measurements of (A) survey, (B) C1s, and (C) S2p spectra over OMR-[C$_3$HMTA][SO$_4$H].

Fig. 5 FT-IR spectra of (a) OMR-[C$_3$HMTA][SO$_4$H] and (b) OMR-[C$_3$HMTA][SO$_3$CF$_3$].
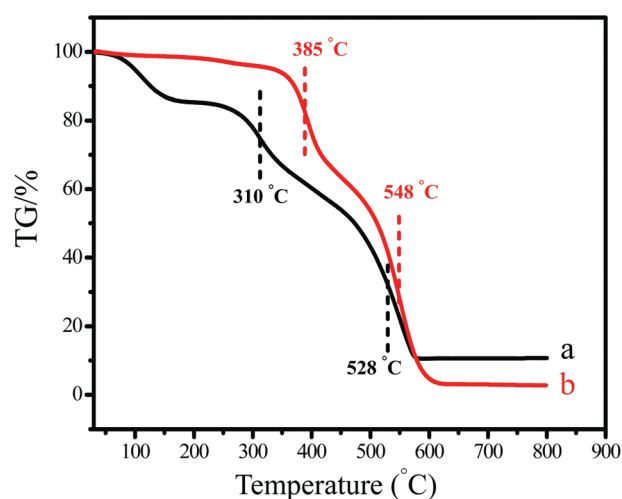
Fig. 6 TG curves of (a) Amberlyst 15 and (b) OMR-[C$_3$HMTA][SO$_3$CF$_3$].
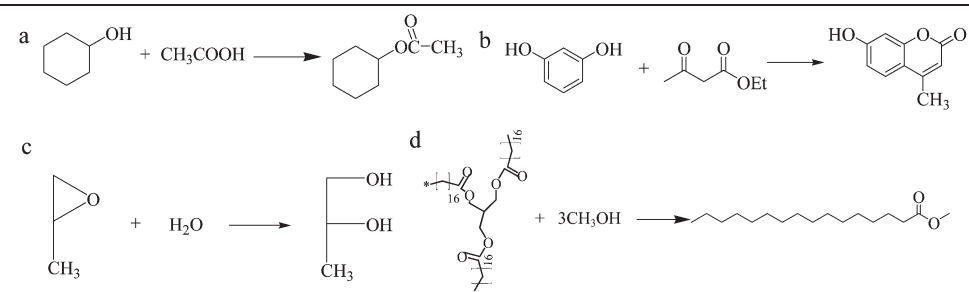
Fig. 7 NH$_3$ TPD curves of (a) OMR-[C$_3$HMTA][SO$_3$CF$_3$] and (b) H-form ZSM-5 zeolite.

[C$_3$HMTA][SO$_3$CF$_3$] would be helpful for their good recyclability in various acid-catalyzed reactions.

Fig. 7 shows the temperature-programmed desorption of ammonia (NH$_3$-TPD) curves of OMR-[C$_3$HMTA][SO$_3$CF$_3$] and the H-form ZSM-5 zeolite, which was an efficient characterization for evaluating the acid strength for solid acids. Clearly, for ZSM-5, the desorption temperature for NH$_3$ was centered at 174 and 448 °C. Interestingly, OMR-[C$_3$HMTA][SO$_3$CF$_3$] showed two peaks centered at 404 and 485 °C respectively, which were much higher than that of the H-form ZSM-5. The obvious higher desorption temperatures of OMR-[C$_3$HMTA][SO$_3$CF$_3$] indicates its stronger acid strength, as compared with that of H-form ZSM-5, which is a typical type of zeolite with a very strong acidit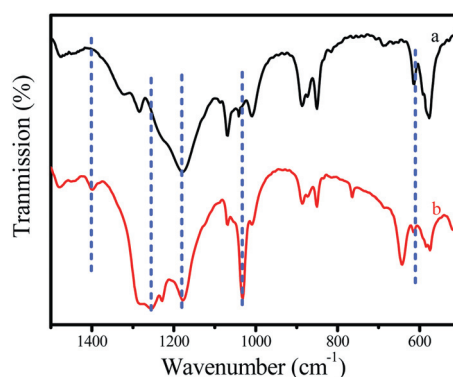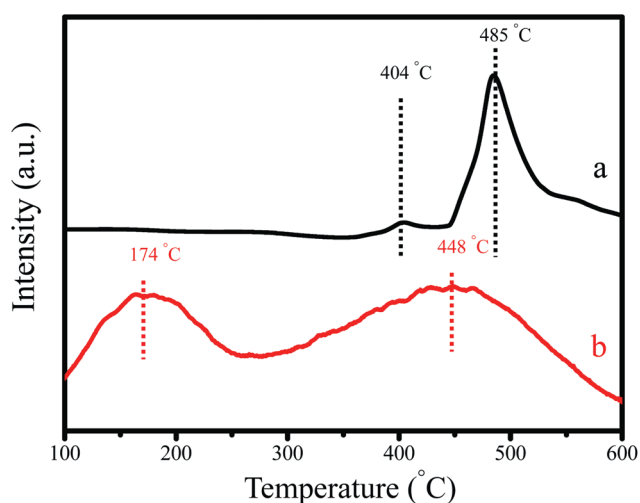y at high temperatures. A stronger acid strength is favorable for obtaining samples with excellent catalytic activities.

Table 2 Catalytic data of the esterification of acetic acid with cyclohexanol (EAC), Peckmann reaction of resorcinol with ethyl acetoacetate (PRE), hydration of propylene oxide water (HPW) and transesterification of tripalmitin with methanol (TTM) over various solid acid catalysts

| Run	Samples	EAC^a conv. (%)	TOF (h^{-1})	PRE^b conv. (%)	TOF (h^{-1})	HPO^c yield (%)	TOF (h^{-1})	TTM^d conv. (%)	TOF (h^{-1})
1	OMR-[C$_3$HMTA][SO$_4$H]	91.2	53	~99	13	94.4	41	98.6	1.4
2	OMR-[C$_3$HMTA][SO$_4$H]^e	90.8	52	98.5	13	92.8	40	94.1	1.3
3	OMR-[C$_3$HMTA][SO$_3$CF$_3$]	93.8	79	~99	19	96.8	62	97.1	1.9
4	Amberlyst 15	62.2	15	80.5	4	51.3	9	61.7	0.3
5	SBA-15-Ar-SO$_3$H	54.5	45	70.3	13	36.7	23	46.3	0.9
6	SBA-15-[C$_3$mim][SO$_3$CF$_3$]	58.7	83	71.2	22	42.8	46	45.7	1.5
7	H-USY	39.8	21	44.7	5	30.1	12	16.7	0.2
8	H-Beta	34.1	31	48.6	10	26.7	18	6.5	0.14
9	H$_2$SO$_4$	94.5	5	~99	1	98.3	4	99.1	0.13

^{a} The activities in EAC were evaluated by cyclohexanol conversion. Reaction temperature: 100 °C, catalyst/cyclohexanol = 0.018. ^{b} The activities in PRE were evaluated by ethyl acetoacetate conversion. Reaction temperature: 110 °C, catalyst/ethyl acetoacetate = 0.154. ^{c} The activities in HPO were evaluated by the yield of 1,2-propylene glycol. Reaction temperature: 27 °C, catalyst/propylene oxide = 0.011. ^{d} The activities in TTM were evaluated by the yield of methyl palmitate. Reaction temperature: 65 °C, catalyst/tripalmitin = 0.0595. ^{e} The catalyst recycled for five times.

Table 2 presents the catalytic data of the esterification of acetic acid with cyclohexanol (EAC), transesterification of tripalmitin with methanol (TTM), Peckmann reaction of resorcinol with ethyl acetoacetate (PRE), and hydration of propylene oxide (HPW) over various catalysts. Clearly, the OMR-ILs samples showed much higher catalytic activities than those of conventional solid acids of Amberlyst 15 (Table 2, run 4), SBA-15-[C$_3$mim][SO$_3$CF$_3$] (Table 2, run 5) and acidic zeolites, which were even comparable with that of homogeneous sulfuric acid. For example, in the reaction of TTM, which is a very important reaction for the production of green and renewable biodiesel under acid catalysis, OMR-ILs samples exhibit yields of biodiesel at 98.6–94.1% (TOF = 1.3–1.9 h^{-1}, Table 2, runs 1 and 3), which are much higher than that of Amberlyst 15 (61.7%, TOF = 0.3 h^{-1}, Table 2, run 4), SBA-15-Ar-SO$_3$H (46.3%, TOF = 0.9 h^{-1}, Table 2, run 5), SBA-15-[C$_3$mim][SO$_3$CF$_3$] (45.7%, TOF = 1.5 h^{-1}, Table 2, run 6) and zeolites (Table 2, runs 7–8, 16.7 and 6.5%, TOF = 0.14–0.2 h^{-1}), which were comparable with that of homogeneous H$_2$SO$_4$ (99.1%, TOF = 0.13 h^{-1}) (Table 2, run 9). Similar results can also be found in other reactions of EAC, PRE, and HPO. For example, OMR-[C$_3$HMTA][SO$_4$H] and OMR-[C$_3$HMTA][SO$_3$CF$_3$] showed the catalytic activities of 91.2 and 93.8%, 99.0 and 99.0%, and 94.4 and 96.8% (Table 2, runs 1 and 3) respectively, which were much higher than that of Amberlyst 15 (62.2, 80.5, and 51.3%, Table 2, run 4), SBA-15-Ar-SO$_3$H (54.5, 70.3, and 36.7%, Table 2, run 5) and SBA-15-[C$_3$mim][SO$_3$CF$_3$] (58.7, 71.2, and

42.8%, Table 2, run 6), and acidic zeolites (34.1 and 39.8%, 44.7 and 48.6% and 30.1 and 26.7%, Table 2, runs 7 and 8), as comparable with that of sulfuric acid (94.5, 99.0, and 98.3%, Table 2, run 9), demonstrating OMR-ILs could be used as efficient heterogeneous acidic ionic liquids catalysts in various acid-catalyzed reactions.

It is worth noting that the OMR-ILs samples exhibit very good recyclability, after being recycled five times, there were no obvious decreases in catalytic activities in these reactions. For example, in the reactions of TTM, OMR-[C$_3$HMTA][SO$_4$H] still provided yields of biodiesel of 94.1% (Table 2, run 2) after being recycled five times, which was even comparable with that of fresh OMR-[C$_3$HMTA][SO$_4$H] (98.6%, Table 2, run 1); Moreover, similar results can also be found in other reactions such as EAC, PRE and HPW, after recycling five times the OMR-[C$_3$HMTA][SO$_4$H] showed catalytic activities of 90.8, 98.5 and 92.8% respectively, which were even comparable with that of fresh OMR-[C$_3$HMTA][SO$_4$H] (91.2, 99.0, and 94.4%), indicating its excellent recyclability. The above results suggested that OMR-ILs were stable enough to act as renewable acidic catalysts, which would be very important for their widely applications.

Fig. 8 shows the catalytic kinetic curves of OMR-[C$_3$HMTA][SO$_3$CF$_3$], Amberlyst 15 and SBA-15-[C$_3$mim][SO$_3$CF$_3$] in the reaction of TTM for production of the clean and renewable energy of biodiesel. Interestingly, OMR-[C$_3$HMTA][SO$_3$CF$_3$] exhibited a much higher catalytic activity than that of Amberlyst
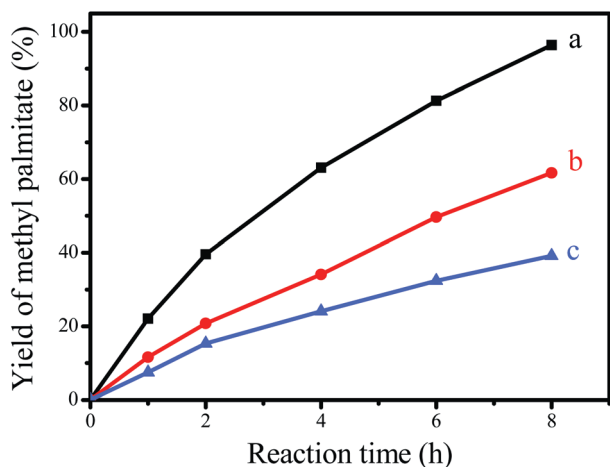
Fig. 8 Catalytic kinetic curves of the transesterification of tripalmitin with methanol over (a) OMR-[C$_3$HMTA][SO$_3$CF$_3$], (b) Amberlyst 15 and (c) SBA-15-[C$_3$mim][SO$_3$CF$_3$].

15 and SBA-15-[C$_3$mim][SO$_3$CF$_3$]. For example, when the reaction lasted for only 4 h, the yield of biodiesel catalyzed by OMR-[C$_3$HMTA][SO$_3$CF$_3$] was up to 63.5%, which is much higher than that of Amberlyst 15 (33.7%) and SBA-15-[C$_3$mim] [SO$_3$CF$_3$] (24.2%); by further increasing the reaction time to 8 h, OMR-[C$_3$HMTA][SO$_3$CF$_3$] showed the yield of biodiesel to be up to 96.8%, however, the yields of biodiesel were only 61.5% and 38.8% when catalyzed by Amberlyst 15 and SBA-15-[C$_3$mim][SO$_3$CF$_3$], which confirms the excellent catalytic performance of OMR-[C$_3$HMTA][SO$_3$CF$_3$]. Therefore, it was reasonably suggested that the excellent catalytic activities of OMR-[C$_3$HMTA][SO$_3$CF$_3$] were attributed to its novel properties of a large BET surface area, strong acid strength, and a stable and adjustable hydrophobic polymeric network.[9,11–15,32,39]

In summary, OMR-ILs which possess a combination of a stable and ordered mesostructure, strong acid strength, excellent catalytic activity together with good recyclability in various acid-catalyzed reactions, will open a new way for the preparation of stable, ordered and efficient mesoporous resin based heterogeneous ionic liquid catalysts for the production of fine chemicals and biomass through green chemical processes.

Conclusions

Strong acidic ionic liquids functionalized, stable and ordered mesoporous resins (OMR-ILs) have been successfully synthesized from the self assembly of phenol–formaldehyde resol with copolymer surfactants in the presence of HMTA crosslinker reagent under high temperature (200 °C) hydrothermal conditions, after calcination for removal of the template, treatment by 1,3-propanesultone, and ion exchanging using various strong acids, OMR-ILs samples were obtained. Interestingly, the OMR-ILs exhibit strong acid strength, high BET surface areas, abundant mesoporosity and adjustable hydrophobic networks, which result in samples with excellent catalytic activities and recyclability in esterification, transesterification, hydration and Peckmann reactions, the excellent acid-catalyzed activities will be potentially important for their widely applications in industry.

Notes and references

1 C. T. Kresge, M. E. Leonowicz, W. J. Roth, J. C. Vartuli and J. S. Beck, *Nature*, 1992, **359**, 710.
2 J. S. Beck, J. C. Vartuli, W. J. Roth, M. E. Leonowicz, C. T. Kresge, K. D. Schmitt, C. T. W. Chu, D. H. Olson and E. W. Sheppard, *J. Am. Chem. Soc.*, 1992, **114**, 10834.
3 Y. Wan and D. Y. Zhao, *Chem. Rev.*, 2007, **107**, 2821.
4 P. D. Yang, D. Y. Zhao, D. I. Margolese, B. F. Chmelka and G. D. Stucky, *Nature*, 1998, **396**, 152.
5 D. Y. Zhao, J. L. Feng, Q. S. Huo, N. Melosh, G. H. Fredrickson, B. F. Chmelka and G. D. Stucky, *Science*, 1998, **279**, 548.
6 J.-L. Blin, A. Léonard, Z.-Y. Yuan, L. Gigot, A. Vantomme, A.-K. Cheetham and B. L. Su, *Angew. Chem., Int. Ed.*, 2003, **42**, 2872.
7 F. Schüth, *Chem. Mater.*, 2001, **13**, 3184.
8 R. Ryoo, S. H. Joo and S. Jun, *J. Phys. Chem. B*, 1999, **103**, 7743.
9 Y. Meng, D. Gu, F. Q. Zhang, Y. F. Shi, H. F. Yang, Z. Li, C. Z. Yu, B. Tu and D. Y. Zhao, *Angew. Chem., Int. Ed.*, 2005, **44**, 7053.
10 B. Z. Tian, X. Liu, B. Tu, C. Z. Yu, J. Fan, L. Wang, S. H. Xie, G. D. Stucky and D. Y. Zhao, *Nat. Mater.*, 2003, **2**, 159.
11 F. Q. Zhang, Y. Meng, D. Gu, Y. Yan, C. Z. Yu, B. Tu and D. Y. Zhao, *J. Am. Chem. Soc.*, 2005, **127**, 13508.
12 Y. Meng, D. Gu, F. Zhang, Y. Shi, L. Cheng, D. Feng, Z. Wu, Z. Chen, Y. Wan, A. Stein and D. Y. Zhao, *Chem. Mater.*, 2006, **18**, 4447.
13 R. L. Liu, Y. F. Shi, Y. Wan, Y. Meng, F. Q. Zhang, D. Gu, Z. X. Chen, B. Tu and D. Y. Zhao, *J. Am. Chem. Soc.*, 2006, **128**, 11652.
14 Y. Wan, Y. F. Shi and D. Y. Zhao, *Chem. Mater.*, 2008, **20**, 932.
15 Y. H. Deng, T. Yu, Y. Wan, Y. F. Shi, Y. Meng, D. Gu, L. J. Zhang, Y. Huang, X. J. Wu and D. Y. Zhao, *J. Am. Chem. Soc.*, 2007, **129**, 1690.
16 E. C. Peters, F. Svec and J. M. J. Frechet, *Adv. Mater.*, 1999, **11**, 1169.
17 Y. Wan, H. Y. Wang, Q. F. Zhang, M. Klingstedt, O. Terasaki and D. Y. Zhao, *J. Am. Chem. Soc.*, 2009, **131**, 4541.
18 B. de Boer, U. Stalmach, H. Nijland and G. Hadziioannou, *Adv. Mater.*, 2000, **12**, 1581.
19 R. Xing, N. Liu, Y. M. Liu, H. H. Wu, Y. W. Jiang, L. Chen, M. Y. He and P. Wu, *Adv. Funct. Mater.*, 2007, **17**, 2455.
20 A. Corma, *Chem. Rev.*, 1995, **95**, 559.
21 A. Corma, *Chem. Rev.*, 1997, **97**, 2373.
22 M. E. Davis, *Nature*, 2002, **417**, 813.
23 M. J. Climent, A. Corma and S. Iborra, *Green Chem.*, 2011, **13**, 520.
24 R. Mokaya and W. Jones, *J. Catal.*, 1997, **172**, 211.
25 C. W. Jones, K. Tsuji and M. E. Davis, *Nature*, 1998, **393**, 52.
26 A. Onda, T. Ochi and K. Yanagisawa, *Green Chem.*, 2008, **10**, 1033.
27 D. E. López, J. G. Goodwin Jr and D. A. Bruce, *J. Catal.*, 2007, **245**, 381.
28 W. Li, Z. J. Jiang, F. Y. Ma, F. Su, L. Chen, S. Q. Zhang and Y. H. Guo, *Green Chem.*, 2010, **12**, 2135.
29 L. L. Xu, Y. H. Wang, X. Yang, J. L. Hu, W. Li and Y. H. Guo, *Green Chem.*, 2009, **11**, 314.
30 G. Busca, *Chem. Rev.*, 2007, **107**, 5366.
31 T. Welton, *Chem. Rev.*, 1999, **99**, 2071.
32 T. Okuhara, *Chem. Rev.*, 2002, **102**, 3641.
33 J. A. Melero, G. D. Stucky, R. V. Griekena and G. Morales, *J. Mater. Chem.*, 2002, **12**, 1664.
34 Q. H. Zhang, S. G. Zhang and Y. Q. Deng, *Green Chem.*, 2011, **13**, 2619.
35 S. M. Coman, M. Florea, V. I. Parvulescu, V. David, A. Medvedovici, D. De vos, P. A. Jacobs, G. Poncelet and P. Grange, *J. Catal.*, 2007, **249**, 359.
36 A. Bordoloi, S. Sahoo, F. Lefebvre and S. B. Halligudi, *J. Catal.*, 2008, **259**, 232.
37 M.-J. Jin, A. Taher, H.-J. Kang, M. Choi and R. Ryoo, *Green Chem.*, 2009, **11**, 309.
38 F. J. Liu, X. J. Meng, Y. L. Zhan, L. M. Ren, F. Nawaz and F. S. Xiao, *J. Catal.*, 2010, **271**, 52.
39 G. Morales, G. Athens, B. F. Chmelka, R. van Grieken and J. A. Melero, *J. Catal.*, 2008, **254**, 205.
40 V. I. Pârvulescu and C. Hardacre, *Chem. Rev.*, 2007, **107**, 2615.
41 A. A. K. Whitehouse, E. G. K. Pritchett and G. Barnett, *Phenolic Resins*, Iliffe, London, 1967.
42 A. Knop and L. A. Pilato, *Phenolic Resin: Chemistry, Application, and Performance, Future Directions*, Springer-Verlag, Berlin, 1985.
43 A. Zinke, *J. Appl. Chem.*, 1951, **1**, 257.
44 G. E. Maciel, I. Chuang and L. Gollob, *Macromolecules*, 1984, **17**, 1081.
45 F. J. Liu, C. J. Li, L. M. Ren, X. J. Meng, H. Zhang and F.-S. Xiao, *J. Mater. Chem.*, 2009, **19**, 7921.

46 D. Margolese, J. A. Melero, S. C. Christiansen, B. F. Chmelka and G. D. Stucky, *Chem. Mater.*, 2000, **12**, 2448.

47 A. S. Amarasekara and O. S. Owereh, *Catal. Commun.*, 2010, **11**, 1072.

48 D. Y. Zhao, Q. S. Huo, J. L. Feng, B. F. Chmelka and G. D. Stucky, *J. Am. Chem. Soc.*, 1998, **120**, 6024.

49 C. Koibeck, M. Killian, F. Maier, N. Paape, P. Wasserscheid and H.-P. Steinrück, *Langmuir*, 2008, **24**, 9500.

50 J. Scaranto, A. P. Charmet and S. Giorgianni, *J. Phys. Chem. C*, 2008, **112**, 9443.

51 N. Asano, M. Aoki, S. Suzuki, K. Miyatake, H. Uchida and M. Watanabe, *J. Am. Chem. Soc.*, 2006, **128**, 1762.

52 H. R. Allcock, T. J. Hartle, J. P. Taylor and N. J. Sunderland, *Macromolecules*, 2001, **34**, 3896.

53 V. Sans, N. Karbass, M. I. Burguete, V. Compañ, E. García-Verdugo, S. V. Luis and M. Pawlak, *Chem.–Eur. J.*, 2011, **17**, 1894.